Supporting information for:

Biowire model of interstitial and focal cardiac fibrosis

Erika Yan Wang[1], Naimeh Rafatian[2,3,#], Yimu Zhao[4,#], Angela Lee[5], Benjamin Fook Lun Lai[1], Rick Xingze Lu[1], Danica Jekic[6], Locke Davenport Huyer[1,4], Ericka J. Knee-Walden[1], Shoumo Bhattacharya[5], Peter H. Backx[2,3,7], and Milica Radisic[1,3,4,*]

1.Institute of Biomaterials and Biomedical Engineering; University of Toronto; Toronto; Ontario, M5S 3G9; Canada.

2.Department of Physiology, Faculty of Medicine; University of Toronto; Toronto; Ontario, M5S 1A8; Canada.

3.Toronto General Research Institute, Toronto; Ontario, M5G 2C4; Canada.

4.Department of Chemical Engineering and Applied Chemistry; University of Toronto; Toronto; Ontario, M5S 3E5; Canada.

5.RDM Division of Cardiovascular Medicine and Wellcome Trust Centre for Human Genetics; University of Oxford; Oxford, OX3 7BN; United Kingdom.

6.McGill University; Montreal, Quebec, H3A 2K6; Canada.

7.Department of Biology; York University; Toronto; Ontario, M3J 1P3; Canada.

#These second authors contributed equally to this work

* Correspondence: Milica Radisic, m.radisic@utoronto.ca

Table of Contents

Figure S1. Force-frequency relationship (FFR) of the normal and fibrotic tissues after 6 weeks of electrical conditioning

Figure S2. Normal and fibrotic models constructed with commercially available iCells to prove linage-independent consistency

Figure S3. Fibrotic tissues exhibit altered action potential profiles compared to the controls

Figure S4. Effects of furin inhibition on extracellular collagen type I deposition with “scar-in-a-jar” model

Figure S5. Tissue excitability and compaction readouts after drug treatment

Figure S6. Sarcomere length measurement and summary of force generation

Figure S7. Immunostaining of Connexin 43 (Cx43) gap-junction protein

Figure S8. Comparison study of collagen deposition in the infarcted rat heart

Figure S1

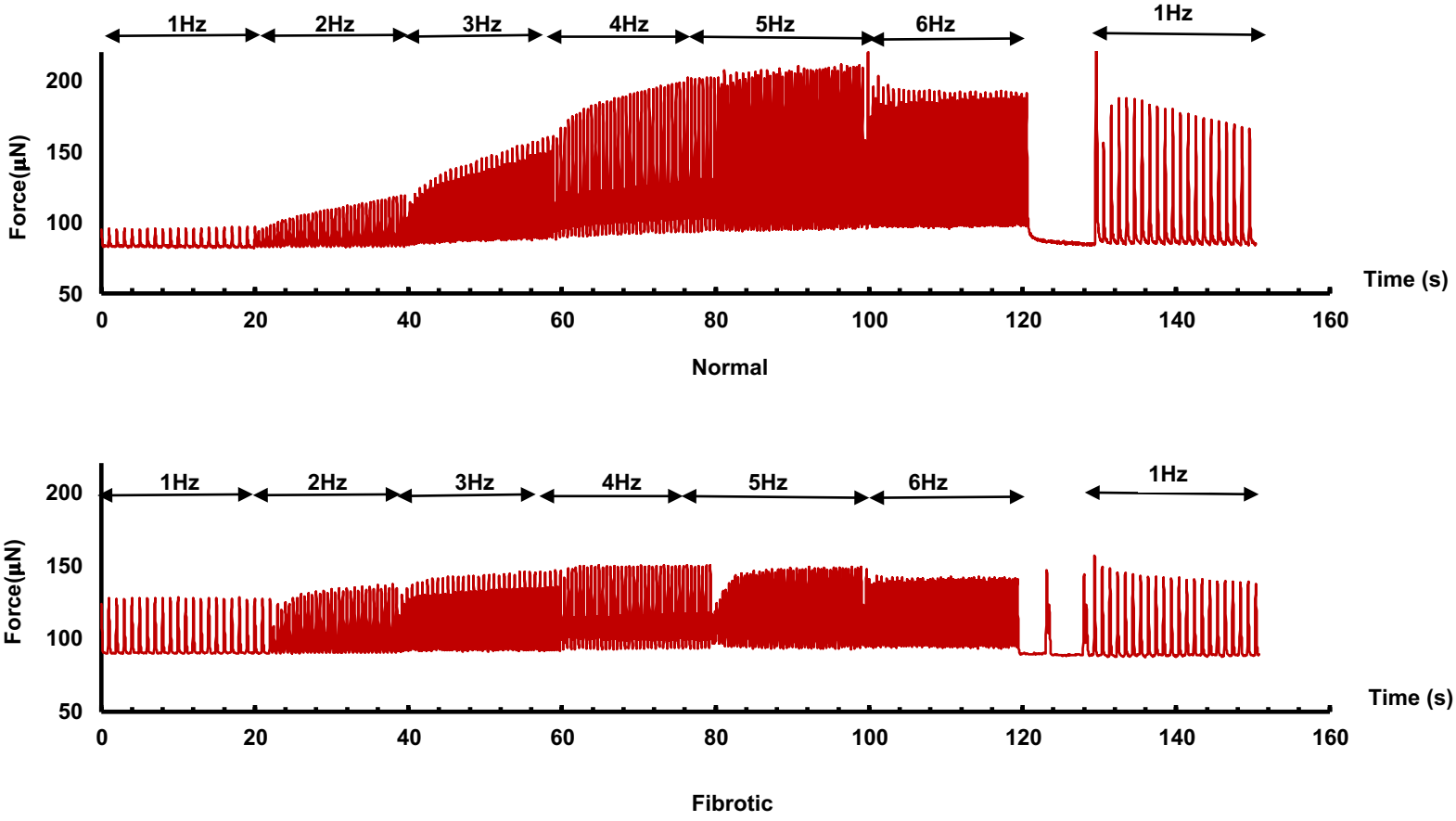

Figure S1. Force-frequency relationship (FFR) of the normal and fibrotic tissues after 6 weeks of electrical conditioning. Tissues were electrically paced from 1-6 Hz. After the last period of high frequency pacing, a short period of rest was induced by turning the stimulator off, followed by re-initiation of pacing at 1Hz to determine post-rest potentiation (PRP) of force.

Figure S2

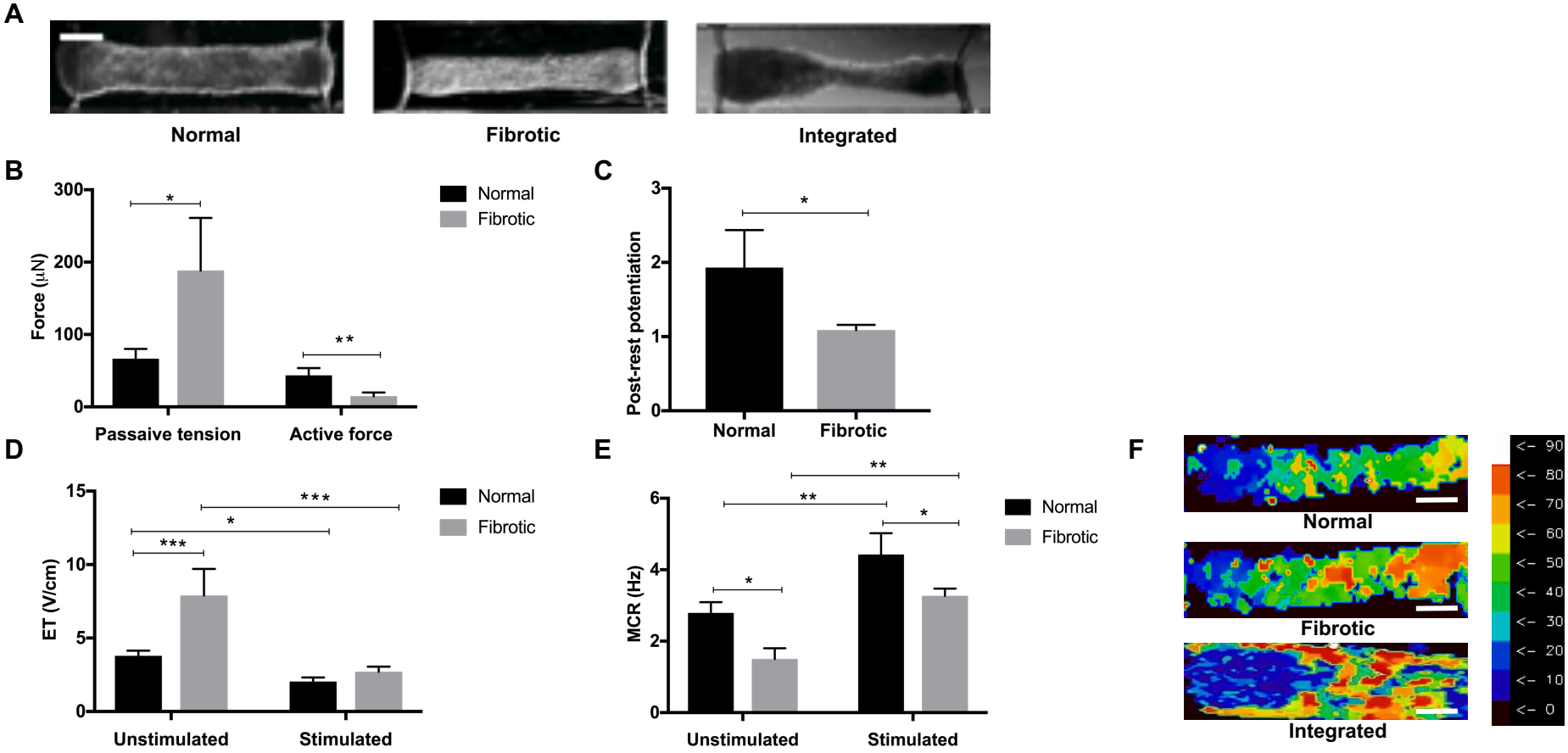

Figure S2. Normal and fibrotic models constructed with commercially available iCells to prove linage-independent consistency. (A) Representative bright field images of normal, fibrotic and integrated tissues constructed using iCells. **(B)** Summary of data for active force and passive tension of normal and fibrotic tissues at electrical stimulation endpoint (mean±SD, n≥3, Student's t test within each group) **(C)** Post-rest potentiation (PRP) of force, normalized to the last pacing frequency, in both groups at maturation endpoint (mean±SD, n≥3, Student's t-test). **(D)** and **(E)** Excitation Threshold (ET) and Maximum Capture Rate (MCR) measurements for unstimulated and stimulated control and fibrotic tissues. (mean±SD, n≥3, two-way ANOVA) **(F)** Conduction velocity maps for normal, fibrotic and integrated tissues constructed with iCells (Scale bar=500 μM). The color scale represents time for electrical pulse to pass through in milliseconds.

Figure S3

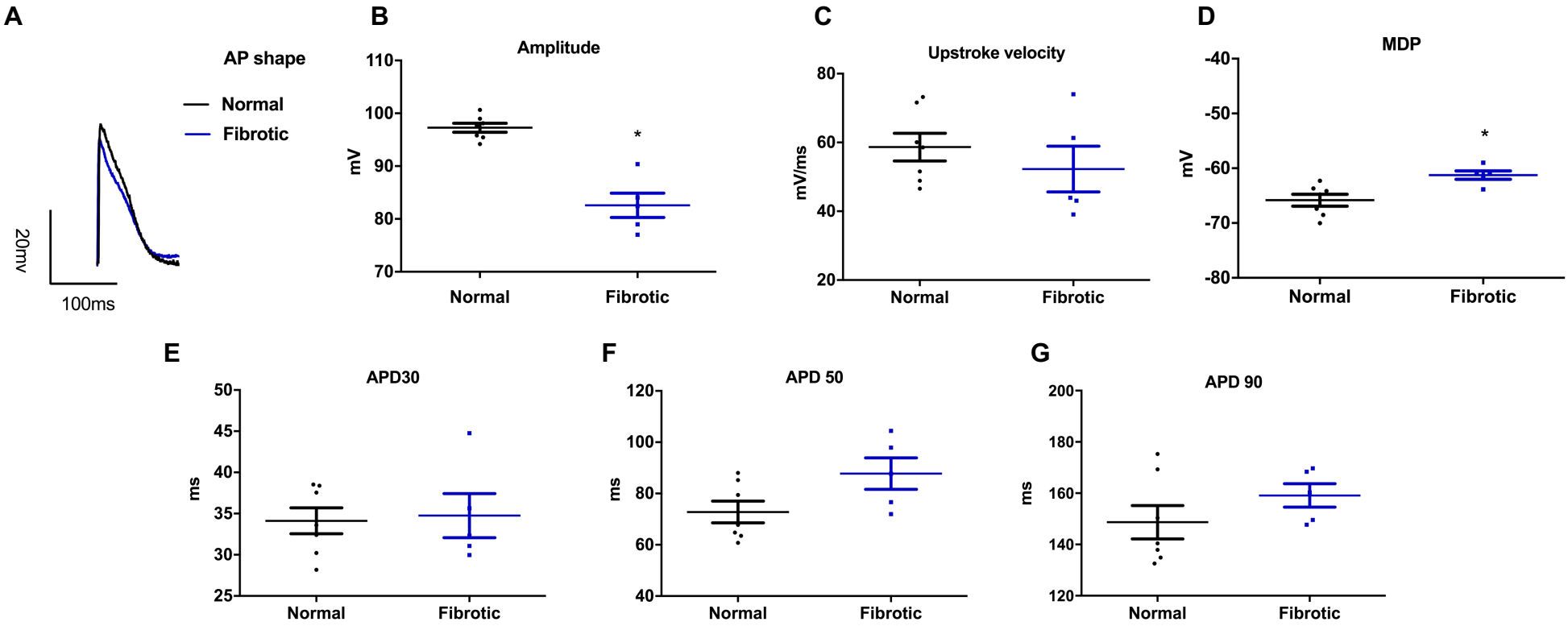

Figure S3. Fibrotic tissues exhibit altered action potential profiles compared to the controls. **(A)** Representative action potential shapes for normal and fibrotic tissues at the end of electrical conditioning. **(B)-(G)** Action potential profiles of normal and fibrotic tissues. Summary of comparisons between two groups for **(B)** action potential amplitudes, **(C)** upstroke velocity, **(D)** maximum diastolic potentials (MDP), **(E)** action potential duration measured at 30% (APD30), **(F)** 50% (APD50) and **(G)** 90% (APD90) repolarization (mean±SD, n≥3, Student's t test).

Figure S4

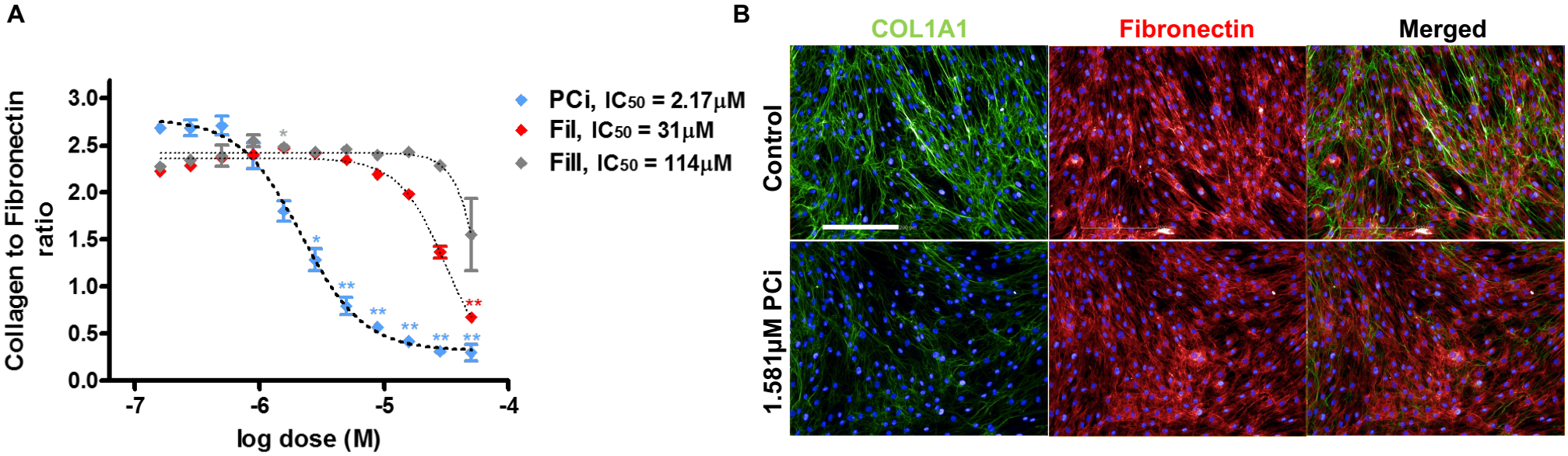

Figure S4. Effects of furin inhibition on extracellular collagen type I deposition with "scar-in-a-jar" model. (A) Inhibitor dose response curves showing collagen to fibronectin ratio versus inhibitor dose for three proprotein convertase inhibitors, PCi, FiI, and FiII. Twelve concentrations in quarter log interval from 50 μM (5×10^{-5} M) to 0.158 μM ($5 \times 10^{-7.5}$ M) were tested. Collagen: fibronectin ratio was calculated from image analysis of anti-Collgen type I and anti-fibronectin immunofluorescence. Dose response curves were fitted by a nonlinear sigmoidal dose response function to a variable slope without constraints, based on which an IC50 for each drug was determined. Data are shown as mean ± SEM, n = 4. The Z-factor for each data point was calculated. *, $0 < Z < 0.5$; **, $0.5 < Z < 1$. **(B)** Immunostaining of Collagen type I and fibronectin with PCI treatment (Scale bar=200 μM).

Figure S5

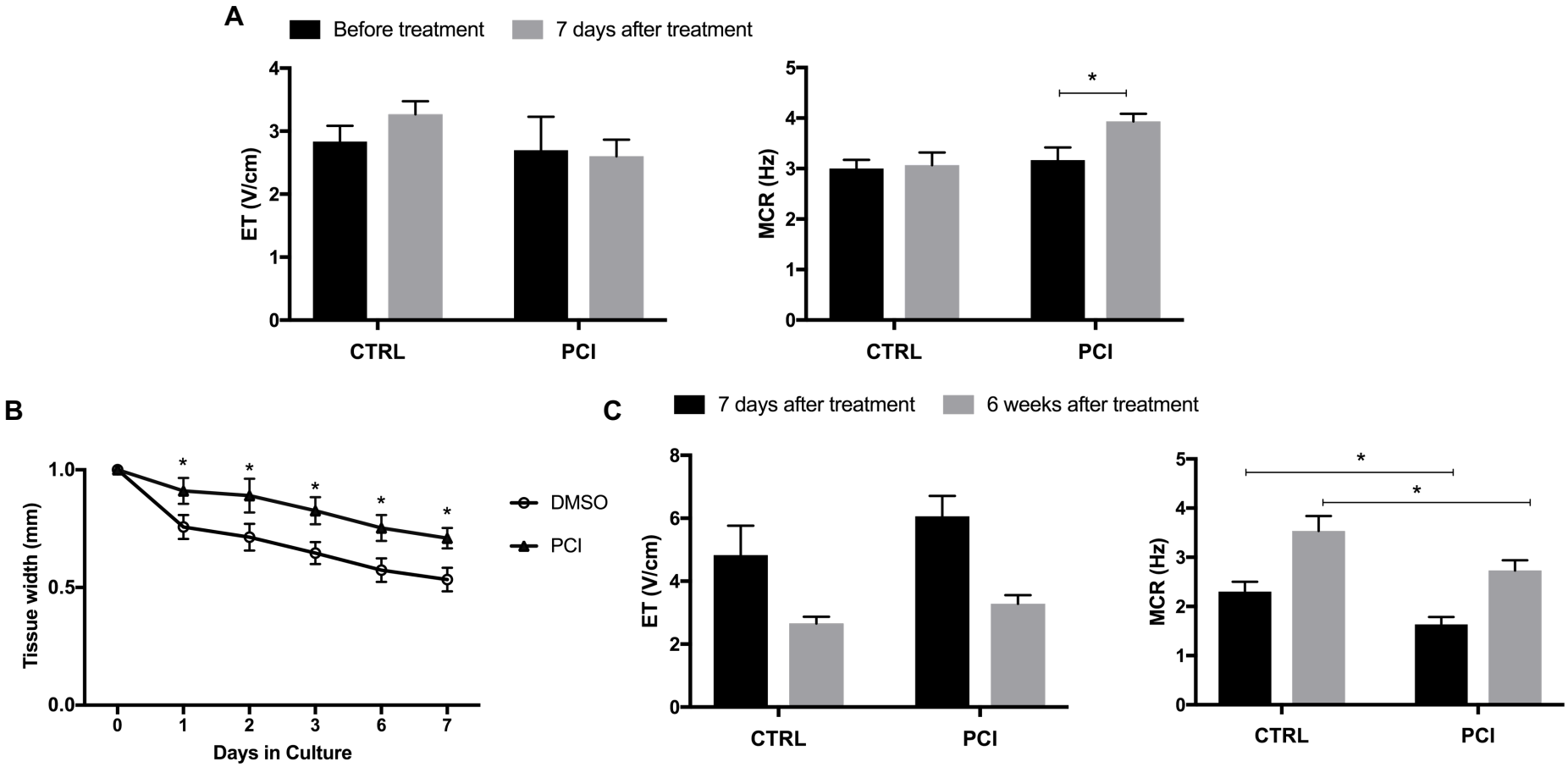

Figure S5. Tissue excitability and compaction readouts after drug treatment. (A) Excitation Threshold (ET) and Maximum Capture Rate (MCR) measurements for PCI treated and control fibrotic Biowire II tissues based on late treatment, Regimen 1 (mean±SD, n≥3, Student's t-test within each group) **(B)** Summary of tissue compaction with PCI treatment compared to control after 7 days of early treatment based on Regimen 2 (mean±SD, n≥3). **(C)** ET and MCR measurements after 7 days and 6 weeks of PCI treatment based on Regimen 2 (mean±SD, n≥3, two-way ANOVA).

Figure S6

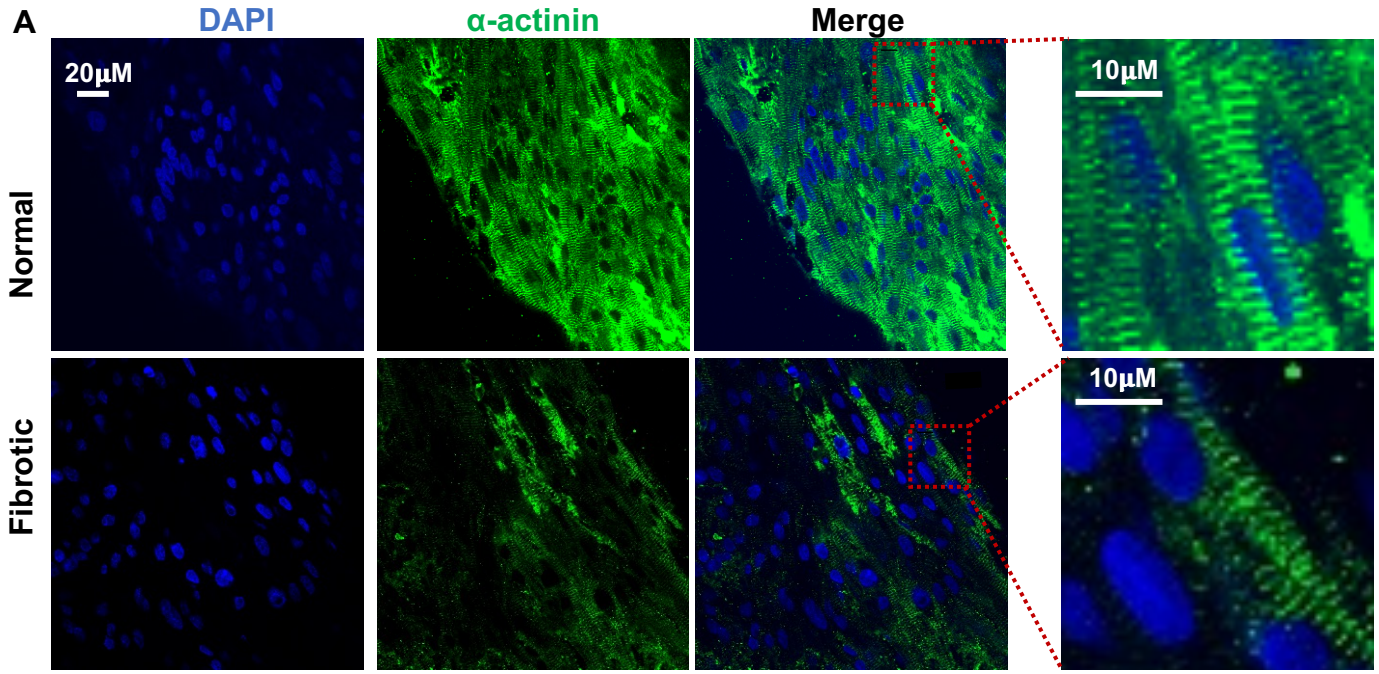

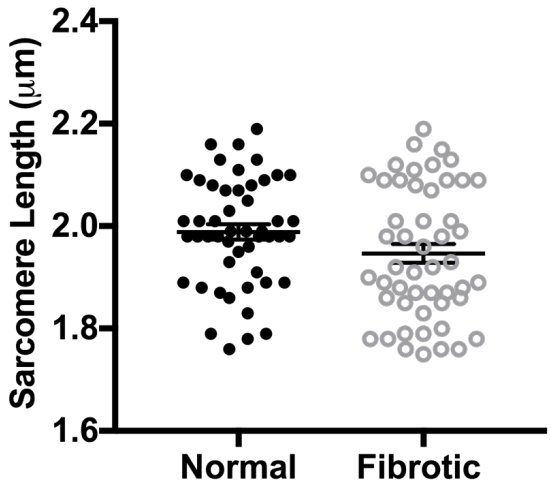

C

	Total CM Number	Active Force (mN)	Active Force (mN/mm²)	Active Force/In put CM (nN/Cell)	Pacing Frequency
Normal	7.5x10⁴	0.011±0.0019	0.055±0.01	0.147±0.025	1Hz
Fibrotic	2.5x10⁴	0.0049±0.0016	0.026±0.009	0.196±0.064	1Hz

Figure S6. Sarcomere length measurement and summary of force generation. (A) Representative immunostaining images of normal and fibrotic tissues at stimulation endpoint stained for sarcomeric α-actinin, and counterstained with the nuclear stain DAPI (Scale bar=20μm). **(B)** Corresponding sarcomere length measured from (A). (mean±SD, n=50, Student's t test). **(C)** A table showing a summary of force generation of normal and fibrotic Biowire tissues with 1Hz pacing (mean±SD, n≥3).

Figure S7

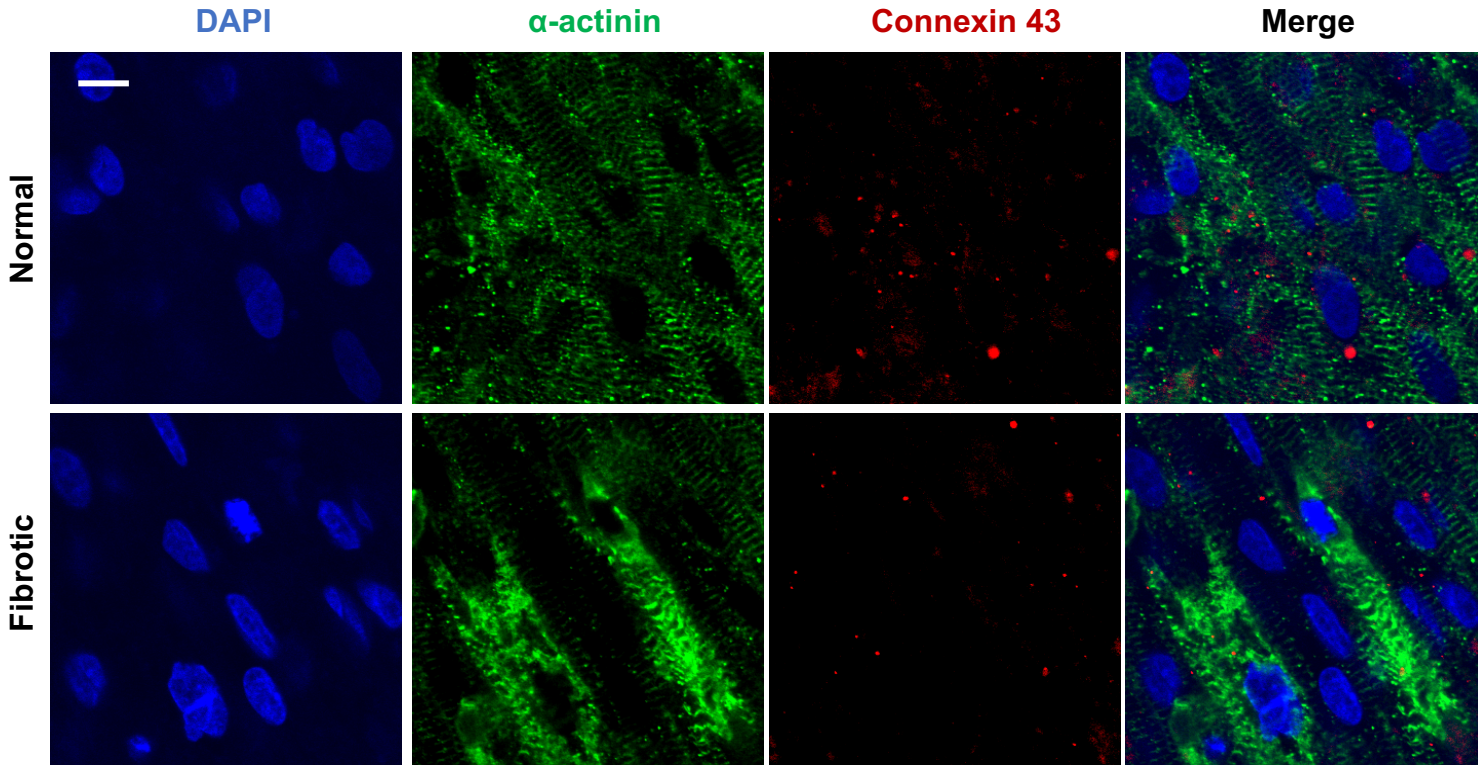

Figure S7. Immunostaining of Connexin 43 (Cx43) gap-junction protein. Representative immunostaining images of normal and fibrotic tissues at stimulation endpoint double-stained for Connexin 43 (Cx-43) and sarcomeric α-actinin, counterstained with the nuclear stain DAPI (Scale bar=10μm).

Figure S8

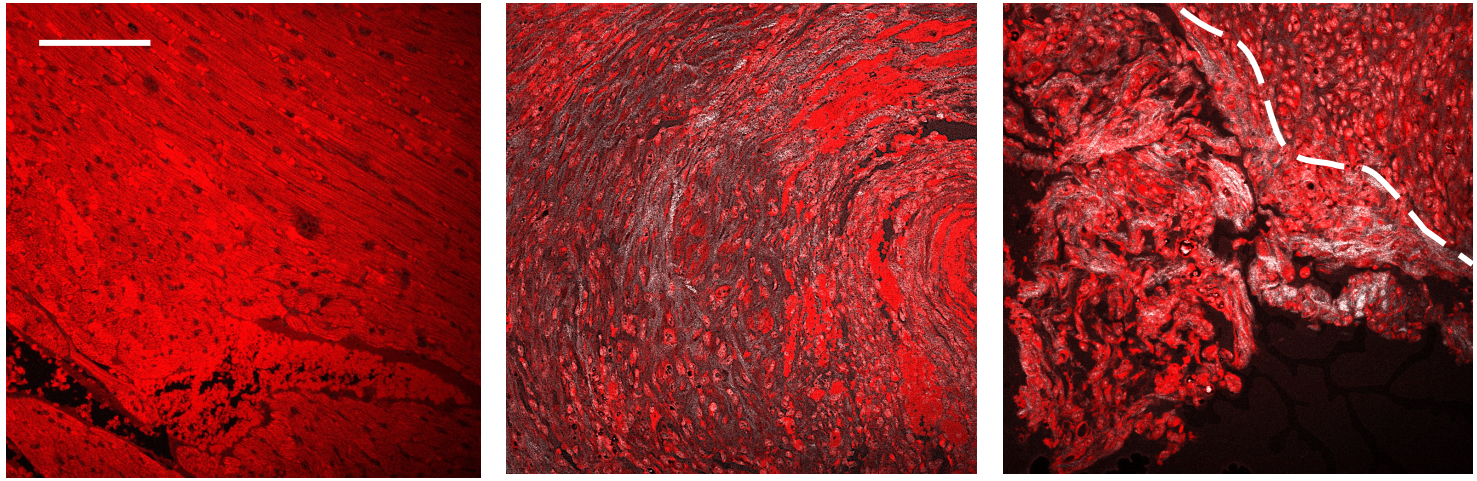

Figure S8. Comparison study of collagen deposition in the infarcted rat heart. Representative secondary harmonic generation images (SHG) with Sham and MI rat cardiac sections. Both interstitial and focal fibrotic lesions are observed in the MI heart (Scale bar=100μm).